Appl Phys A (2010) 99: 797–803
DOI 10.1007/s00339-010-5745-6

Applied Physics A
Materials Science & Processing

Growth fusion of submicron spherical boron carbide particles by repetitive pulsed laser irradiation in liquid media

Yoshie Ishikawa · Qi Feng · Naoto Koshizaki

Received: 6 January 2010 / Accepted: 22 April 2010 / Published online: 21 May 2010

Abstract We studied the fabrication of B_4C submicron particles by laser irradiation of boron nanoparticles dispersed in an organic solvent. The spherical shape of the formed particles suggests that instantaneous melt formation and solidification by quenching are involved in the particle-forming process. B_4C particles gradually became larger with irradiation time at relatively low laser fluence (1.5 J cm^{-2} pulse^{-1}) by repetitive melting and fusion of the particles, and the B_4C yield increased with irradiation time to 90% for 600 min of irradiation. At higher laser fluences, the B_4C yield decreased due to the explosive ablation of boron or B_4C to form H_3BO_3, and thus only the larger B_4C particles were observed. The dielectric constant of the organic solvent also affected the generated B_4C particle size, probably due to the degree of particle aggregation. Thus, this technique can provide a new approach for fabricating spherical submicron particles of ceramic materials, such as carbides, with simple and safe processes.

1 Introduction

Laser ablation in a liquid environment is of considerable interest as a new tool for preparing nanoparticles. Pioneering work by Patil, Henglein, and others proved the possibility of nanoparticle fabrication by quenching [1–3]. Mafuné et al. introduced a chemical approach to laser ablation in liquid by reporting the surfactant effects on noble metal nanoparticle formation in water by laser ablation of bulk noble metal [4], and their work triggered the application of this technique to various material systems. For example, crystallized oxide nanoparticles such as SnO_2, TiO_2, and ZnO can be easily obtained at room temperature by ablating a bulk target of reactive metal such as Sn, Ti, or Zn in surfactant aqueous solution exceeding the critical micelle concentration without subsequent heat treatment [5–7]. Nanoparticles of nitride or carbide, such as C_3N_4, TiN, or TiC, were also recently reported to be formed by laser ablation of bulk graphite or titanium metal in a liquid containing N or C atoms [8–10]. Thus, this process is applicable to fabricating various nanoparticles including novel exotic nanomaterials. Simplicity and inexpensive equipment for controlling the ablation atmosphere are also advantages of this process over conventional nanoparticle-preparation methods.

In the above cases, bulk solid targets were used as the raw material for fabricating nanoparticles. However, the production of nanoparticles during laser ablation in liquid is gradually suppressed due to the shadowing of laser energy onto the target fixed on the bottom of an irradiation vessel by generated nanoparticles. Powder dispersed in liquid has recently been used as a target to effectively apply the laser energy to the target and to improve the product yield by reducing the shadowing effect. In such a case, irradiated laser energy mostly induces fragmentation of particles, splash of melts instantaneously formed from particles, and ablation of target material from particles, resulting in the gradual size reduction of generated particles with laser irradiation time to several nanometers or several tens of nanometers.

We previously reported fabricating spherical boron carbide (B_4C) submicron particles by irradiating a laser beam

Y. Ishikawa · Q. Feng
Department of Advanced Materials Science, Faculty of Engineering, Kagawa University, 2217-20 Hayashi-cho, Takamatsu, Kagawa 761-0396, Japan

N. Koshizaki (✉)
Nanosystem Research Institute (NRI), National Institute of Advanced Industrial Science and Technology (AIST), Central 5, 1-1-1 Higashi, Tsukuba, Ibaraki 305-8565, Japan
e-mail: koshizaki.naoto@aist.go.jp

at a relatively weak fluence onto boron nanoparticles (50–100 nm) dispersed in ethyl acetate through the reaction between the boron particles and the carbon component in the ethyl acetate [11]. The spherical particle shape suggests that particles are first melted and then solidified by quenching. It is noteworthy that the B_4C particles thus obtained are larger than raw B particles, and increase in size with laser irradiation time, probably by fusion of melted particles. These results of increasing particle size are contrary to those of many past reports on laser irradiation in liquid using powder targets, as explained above [12, 13]. Only a limited number of studies reported the formation of a few larger particles by this method [14], although a large number of smaller particles were simultaneously observed in the product.

Recently, B_4C spherical particles have been proposed as a candidate agent for boron neutron capture therapy (BNCT) utilizing tumor destruction by α particles produced by nuclear division of ^{10}B ingested in the tumor cells [15]. Laser irradiation in liquid may be a promising approach for fabricating B_4C submicron particles with spherical shape, since conventional fabrication processes of B_4C particles can only provide shapeless forms with a high possibility of contamination due to the B_4C characteristics as a high-temperature ceramic material (melting point 2350°C) with extreme hardness [16–18].

Thus, understanding the formation process and mechanism of spherical submicron B_4C particles is important for developing a general method of fabricating submicron spherical particles in a new application field. We report herein the detailed mechanism of B_4C particle fusion growth and effects of laser irradiation time, laser fluence, and solvent on the particle growth. This report will extend the range of available particle size by laser processing in liquid, and develop a new type of application using high-temperature ceramic particles that are difficult to obtain by conventional processing techniques.

2 Experimental

Reagent-grade B powder (0.24 mg, 99.995%; Aldrich Chemical Company, Inc.) was dispersed in 6 ml ethyl acetate (99.5%, Wako Pure Chemical Industries, Ltd.), ethanol (99.5%, Wako Pure Chemical Industries, Ltd.), methanol (99.8%, Wako Pure Chemical Industries, Ltd.), 1-propanol (99.5%, Tokyo Kasei Kogyo Co., Ltd.), acetone (99.0%, Wako Pure Chemical Industries, Ltd.), acetonitrile (99.5%, Wako Pure Chemical Industries, Ltd.), or *N*,*N*-dimethylformamide (DMF) (infinity pure, Wako Pure Chemical Industries, Ltd.) in a glass vessel. The B powder in the solvent was then irradiated with the third harmonic (355 nm) of a Nd:YAG laser operated at 10 Hz with a pulse width of 7 ns for various irradiation times and at various fluences. The laser beam was focused 2 mm below the suspension surface, using a lens with a focal length of 50 mm. The suspension was agitated using a magnetic stirrer during irradiation. The experimental configuration for laser irradiation of B particles is illustrated in Fig. 1. The particles obtained by laser irradiation of B were treated with HNO_3 using the following procedure to remove unreacted B and by-product H_3BO_3. First, the solvents were completely evaporated using a centrifugal evaporator, and then the obtained particles were dispersed in 6.2 M HNO_3 for 24 h. During this treatment, the B and H_3BO_3 were completely dissolved in the HNO_3, whereas the B_4C particles remained undissolved. The B_4C particles were subsequently separated from the supernatant by centrifugation. The B concentrations of the supernatants were then analyzed for B_4C yield evaluation using inductively coupled plasma optical emission spectrometry (ICP-OES) measurements. At the same time, the collected B_4C particles were repeatedly rinsed with deionized water and centrifuged to remove HNO_3. The as-prepared suspension and a suspension taken after the HNO_3 treatment were dropped onto a Si substrate and dried in air in preparation for X-ray powder diffraction analysis (XRD; Rigaku RAD-C) with Cu Kα radiation and morphology observation by a field emission scanning electron microscope (SEM; Hitachi S4800). The particles treated with HNO_3 were also mounted on a carbon-coated grid for transmission electron microscope (TEM; JEOL JEM 2010) observation. The mean size of the particles was determined by measuring the diameters of 200 particles in SEM images.

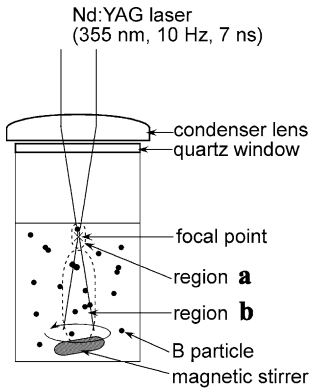

Fig. 1 Experimental configuration for laser irradiation of B particles dispersed in organic solvent. *Region (a)* is near the focal point in the suspension. *Region (b)* is far below the focal point, in which incident laser light is attenuated due to absorption and scattering by particles in the light path

3 Results and discussion

3.1 Effect of laser irradiation time on B_4C particle growth and growth mechanism

Boron particles dispersed in ethyl acetate were irradiated at 1.5 J cm^{-2} pulse^{-1} for various irradiation times to investigate the effect of laser irradiation time on B_4C particle for-

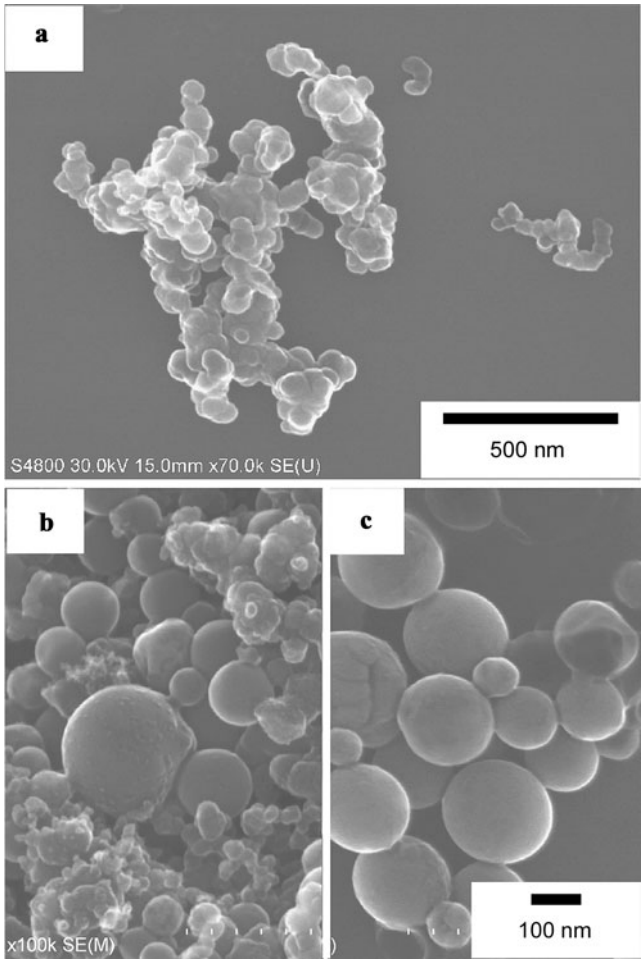

Fig. 2 SEM images of particles before and after laser irradiation at 1.5 J cm^{-2} pulse^{-1} in ethyl acetate. (**a**) Particles before laser irradiation. (**b**) Particles after laser irradiation for 10 min. (**c**) Particles obtained after laser irradiation for 10 min and subsequent HNO_3 treatment

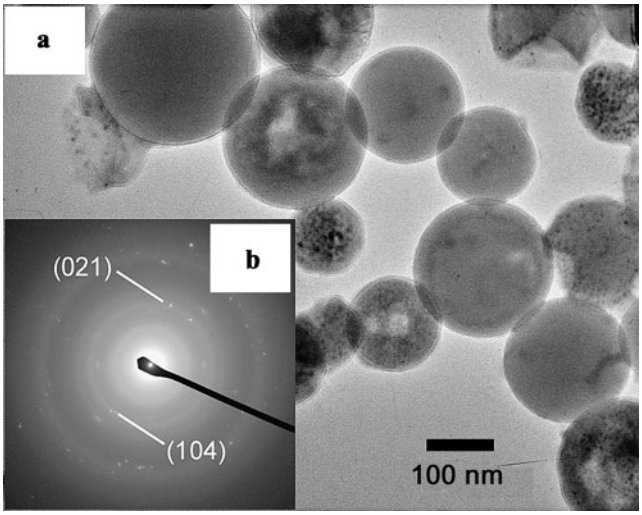

Fig. 3 (**a**) TEM image and (**b**) selected area electron diffraction pattern for particles obtained by laser irradiation at 1.5 J cm^{-2} pulse^{-1} in ethyl acetate for 10 min and subsequent HNO_3 treatment

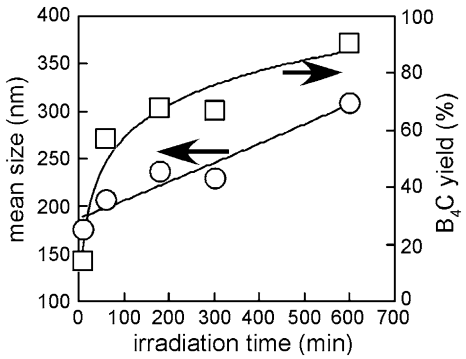

Fig. 4 Laser irradiation time dependence of mean size and yield of B_4C particles prepared by laser irradiation in ethyl acetate at 1.5 J cm^{-2} pulse^{-1}

mation. Figure 2 presents SEM images of (a) raw B particles and (b) particles after laser irradiation in ethyl acetate at 1.5 J cm^{-2} pulse^{-1} for 10 min. Connected irregular grains from 50 to 100 nm were observed in the particles before laser irradiation. In contrast, spherical submicron particles were observed among the raw B particles after laser irradiation (Fig. 2b). Figure 2c depicts particles obtained by laser irradiation under the same conditions as in Fig. 2b and subsequent HNO_3 treatment. Unreacted raw B grains were removed by the HNO_3 treatment, whereas spherical particles remained even after the HNO_3 treatment. Figure 3 presents a TEM image of these remaining particles, and a selected area electron diffraction pattern from these is depicted in the inset in Fig. 3b. These electron diffraction patterns from obtained particles were identified as B_4C. Similar spherical B_4C particles were obtained using various laser irradiation times. Figure 4 plots the relationship between irradiation time and B_4C yield, estimated from the amount of dissolved B components in the subsequent HNO_3 treatment, obtained by laser irradiation in ethyl acetate at 1.5 J cm^{-2} pulse^{-1}. B_4C yields increased with the laser irradiation time. Figure 4 also indicates the relationship between the irradiation time and the mean size of the obtained particles after HNO_3 treatment. The mean particle size increased moderately with irradiation time.

Figure 5 illustrates the scheme of a B_4C formation mechanism by laser irradiation. First, raw B particles irradiated with a laser pulse (Fig. 5a) are melted and fuse to form a submicron B droplet by laser heating, as seen in Fig. 5b. The absorbed photon energy, calculated in a previous report [11], is sufficient to melt the B particles by laser irradiation, even at 1.5 J cm^{-2} pulse^{-1}. Active C species, in radical and/or ionic states, are formed by thermal or photon-induced decomposition of ethyl acetate molecules surrounding the B droplets (Fig. 5b). In addition, unstable atomic, radical, and ionic B species, which cause H_3BO_3 formation, are re-

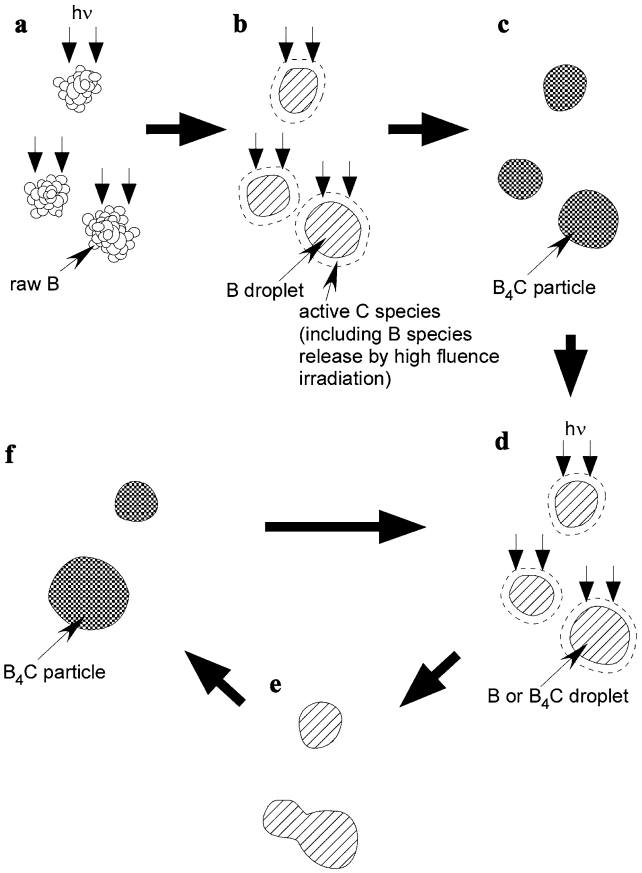

Fig. 5 Scheme of spherical B_4C particle formation mechanism by laser irradiation in ethyl acetate. (**a**) Laser-irradiated raw B particles. (**b**) B droplets melted by laser irradiation with active C species formation, including release of unstable B species by high laser fluence irradiation. (**c**) B_4C particle formation by dissolution of C species into B droplets. (**d**) B or B_4C droplets formed by repetitive laser pulse irradiation. Some droplets fused (**e**), and then (**f**) large B_4C particle formation proceeded

leased by ablation from the irradiated B surface under laser irradiation with relatively high fluence, as discussed in the next subsection. The release of unstable B species is completed within several hundred nanoseconds after the laser pulse irradiation [19], and then the active C species probably dissolve into melted B droplets, forming B_4C crystallites (Fig. 5c). The formed B_4C particles are repeatedly irradiated and melted during each irradiation time (Fig. 5d). The difference in transmittance at the irradiation laser wavelength of a suspension of raw B and that after laser irradiation, in which the B_4C yield was approx. 90%, was only 8%. Therefore, it is probably unlikely to selectively modify only B. Some droplets fuse with each other to form large droplets (Fig. 5e), leading to large spherical B_4C particles (Fig. 5f). The increase in particle mean size with irradiation time (Fig. 4) is due to the repeated fusion of droplets (i.e. the processes in Fig. 5d–f). Mafuné et al. reported similar particle growth by repetitive irradiation of Au nanoparticles at 532 nm [20], and Amendola and Meneghetti mentioned weak-fluence importance for Au nanoparticle growth [21]. An effect of laser fluence on B_4C particle growth is investigated and discussed in the next subsection. The B_4C yield increase is moderated with a further extension of the irradiation time due to consumption of raw B by B_4C formation.

3.2 Effect of laser fluence on B_4C particle growth

Figure 6 presents the SEM images of the particles obtained by irradiation in ethyl acetate at various fluences and subsequent HNO_3 treatment. Laser irradiation at all fluences gave submicron spherical B_4C particles (Fig. 6a–c). Insets in each SEM image are the particle size distributions of particles obtained at each fluence. At the lowest fluence, most particles are 100–400 nm in diameter. As the fluence increases, these values shift to larger diameters. At the highest fluence, particles smaller than 200 nm are not observed and particles greater than 300 nm predominate. Figure 7 illustrates the laser fluence dependence of the mean particle size. The mean particle size increased with an increase of laser fluence, although the mean particle sizes of noble metals and metal oxides are usually reported to decrease with increasing fluence [12, 13].

The evaluated B_4C yields obtained at various fluences are also depicted in Fig. 7. The yield decreased with increasing laser fluence. The XRD patterns of the particles before and after the laser irradiation of B particles in ethyl acetate at various laser fluences, without HNO_3 treatment, are illustrated in Fig. 8. Boron particles were amorphous before the laser irradiation (Fig. 8a). Only B_4C peaks were observed from the particles obtained at 1.5 $J\,cm^{-2}\,pulse^{-1}$ (Fig. 8b). H_3BO_3 peaks appeared with increasing of the laser fluence, as seen in Fig. 8c (5.1 $J\,cm^{-2}\,pulse^{-1}$) and Fig. 8d (25.5 $J\,cm^{-2}\,pulse^{-1}$). Thus, the decrease in B_4C yield at high laser fluence is due to the formation of H_3BO_3 phase.

According to these results, laser irradiation at relatively low fluence ($\sim$1.5 $J\,cm^{-2}\,pulse^{-1}$) is important for preferential B_4C formation; in contrast, irradiation at high fluence causes intensive ablation of B, and unstable B species release explosively from the B particles and/or droplets (the process in Fig. 5b). Although similar behavior also occurs with laser irradiation of noble metal and metal oxide particles at high fluence, in those cases it is followed by nuclei formation, cluster growth, and subsequent formation of nanoparticles whose size is smaller than that of the raw particles [12, 13, 21]. In the case of B_4C, however, B species released by irradiation at high fluence easily react with O species from dissociated ethyl acetate molecules and/or oxygen gas dissolved in solvent to give B_2O_3 and/or H_3BO_3, which are finally removed by HNO_3 treatment. Small B and formed B_4C particles (<200 nm) also disappeared by the explosive B ablation, as shown in Fig. 6c. The ablation probably occurred near the focal point in the suspension (region

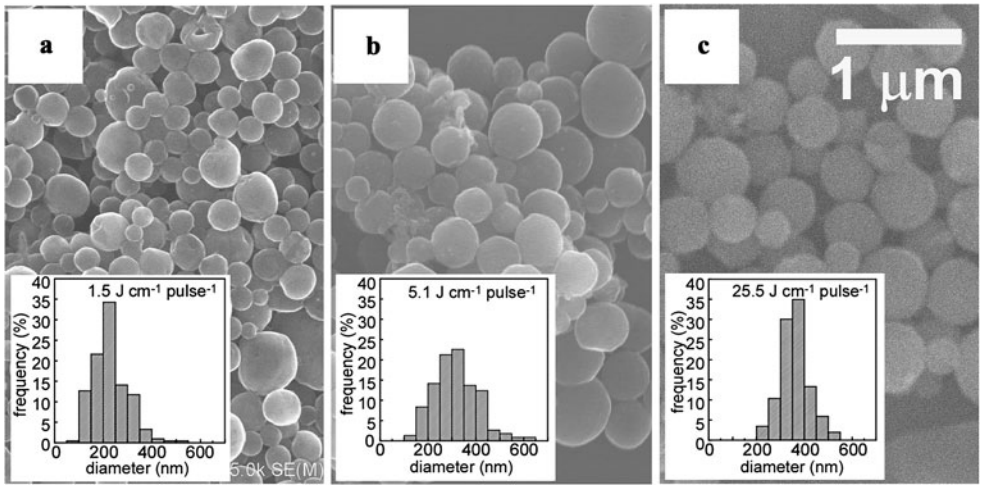

Fig. 6 SEM images of particles obtained by laser irradiation in ethyl acetate for 300 min at various fluences: (**a**) 1.5 J cm^{-2} pulse^{-1}; (**b**) 5.1 J cm^{-2} pulse^{-1}; and (**c**) 25.5 J cm^{-2} pulse^{-1} with subsequent HNO_3 treatment. Insets are corresponding particle size distributions.

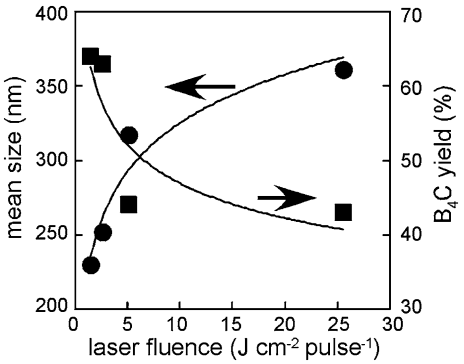

Fig. 7 Laser fluence dependence of the mean size and yield of B_4C particles prepared by laser irradiation for 300 min in ethyl acetate

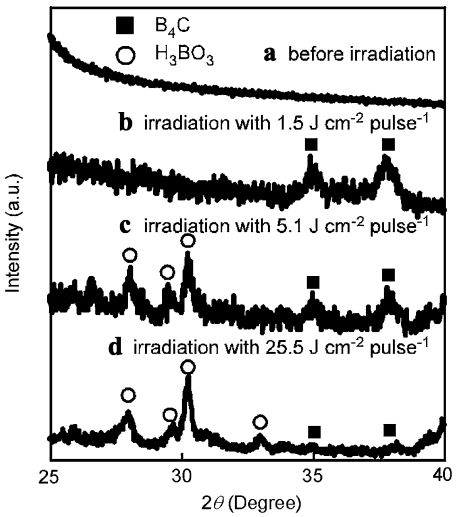

Fig. 8 X-ray powder diffraction spectra of (**a**) particles before irradiation and those after laser irradiation in ethyl acetate for 300 min at (**b**) 1.5 J cm^{-2} pulse^{-1}, (**c**) 5.1 J cm^{-2} pulse^{-1}, and (**d**) 25.5 J cm^{-2} pulse^{-1} without subsequent HNO_3 treatment

(a) in Fig. 1). At the same time, submicron B_4C particles also formed far below the focal point (region (b) in Fig. 1), because raw B and formed B_4C particles irradiated at low fluence (~1.5 J cm^{-2} pulse^{-1}) melted without ablation due to extinction of laser light with increasing optical length in the suspension. The appropriate space for B_4C particle formation in the suspension may be considerably large, and B_4C particles there can recurrently melt, fuse with one another, and give large particles, leading to large mean size. Consequently, selectively large B_4C particles formed with decreasing B_4C yield by relatively high fluence in this irradiation system.

3.3 Effect of liquid medium on B_4C particle formation

Similar spherical B_4C particles are also obtained in ethanol, methanol, 1-propanol, acetone, acetonitrile, and DMF by laser irradiation at 1.5 J cm^{-2} pulse^{-1} for 180 min. The mean particle sizes obtained in these solvents are summarized in Table 1. Solvent parameters may contribute to the mean size, and so the following are also listed in the table: boiling point t_b, enthalpy of vaporization $\Delta_{vap}H$, dielectric constant ε, specific heat capacity c_p, and thermal conductivity k_l [22]. However, it is unlikely that t_b, $\Delta_{vap}H$, c_p, or k_l contributes to the mean size.

Figure 9 shows a plot of mean particle size as a function of solvent dielectric constant ε. The numbers in the figure correspond to those in Table 1. The mean size roughly decreased with increasing dielectric constant. The effect of solvent dielectric constant on particle dispersibility in nonaqueous media has been elucidated using Derjaguin, Landau, Verwey, and Overbeek theory (DLVO theory), in which particles in solvent aggregate with decreasing ε [23]. The particle aggregation behavior depending on ε was also empirically reported [24, 25]. Similarly in our case, raw B and formed B_4C particles are probably aggregated in a solvent with low dielectric constant due to weak solvation force to the particle surface. When the aggregated particles are irra-

Table 1 Features of B_4C particles obtained at 1.5 J cm^{-2} pulse^{-1} for 180 min in various solvents and physical constants of solvents

No.	Solvent	Mean particle size (nm)	Boiling point t_b (°C)[a]	Enthalpy of vaporization $\Delta_{vap}H$ (kJ/mol) at 25°C[a]	Dielectric constant ε at 20°C[a]	Specific heat capacity c_p (J g^{-1} K^{-1}) at 25°C[a]	Thermal conductivity k_l (W m^{-1} K^{-1})°C[a]
1	Ethyl acetate	237	77.3	35.6	6.0814	1.94	0.144
2	Ethanol	181	78.2	42.32	25.3	2.44	0.169
3	Methanol	180	64.6	37.43	33.0	2.53	0.200
4	1-propanol	172	97.2	47.45	20.8	2.39	0.154
5	Acetone	160	56.05	30.99	21.01	2.18	0.161
6	Acetonitrile	142	81.8	32.94	36.64	2.23	0.188
7	*N*,*N*-dimethyl-formamide	147	153	46.89	38.25	2.06	0.184

[a]Ref. [22]

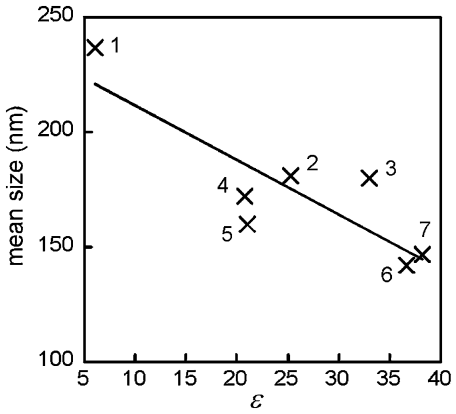

Fig. 9 Dielectric constant dependence of the mean size of B_4C particles prepared by laser irradiation at 1.5 J cm^{-2} pulse^{-1} for 180 min in various solvents. Indicated numbers correspond to those in Table 1

diated by a laser, large B droplets are formed through melting, fusion, and reaction of aggregated particles, resulting in large B_4C particle formation. Particle growth by laser irradiation in liquid was previously reported for the formation of smaller Au nanoparticles (<100 nm) using an aqueous solution of KCl and tetrahydrofuran (THF) to lower the dielectric constant of the solvent [26]. In this study, similar particle growth is observed even for the particles with submicron-scale size. However, compared with mean particle sizes of aliphatic alcohols (ethanol, methanol, and 1-propanol), the effect of dielectric constant on particle size is not observed. Because the chemical property of the solvent molecule may affect the B_4C particle formation, further detailed investigation is required.

4 Conclusions

In conclusion, the sizes and yields of spherical B_4C particles obtained by irradiation in ethyl acetate are affected by laser irradiation time and fluence. The raw B particles melted by laser irradiation and fused with one another into large B droplets. Active C species form by decomposition of ethyl acetate molecules surrounding the droplets, and dissolve in the droplets to form spherical submicron B_4C particles. Irradiation at low fluence (~1.5 J cm^{-2} pulse^{-1}) for long periods brought about preferential B_4C particle growth by repetitive droplet fusion. The B_4C yield decreased with increase of laser fluence due to intensive ablation of B. The ablation occurred near the focal point in the suspension, and finally brought about H_3BO_3 formation. Small particles irradiated with high fluence disappeared by explosive B ejection in this region. On the other hand, B_4C predominantly formed far below the focal point, in which particles were irradiated with moderate-fluence laser light. Consequently, large particles selectively formed with the B_4C yield decreasing under irradiation at high fluence. Moreover, the mean size of the obtained B_4C particles depends on the dielectric constant of the solvent used as a dispersing medium, and decreases with increasing dielectric constant.

Acknowledgements This study was supported by the Research for Promoting Technology Seeds of the Japan Science and Technology Agency and a Grant-in-Aid for Young Scientists (Start-up) of the Japan Society for the Promotion of Science. Part of this study was supported by the Budget for Nuclear Research of the Ministry of Education, Culture, Sports, Science and Technology, based on screening and counseling by the Atomic Energy Commission and a Grant-in-Aid for Scientific Research (B) of the Japan Society for the Promotion of Science.

References

1. P.P. Patil, D.M. Phase, S.A. Kulkarni, S.V. Ghaisas, S.K. Kulkarni, S.M. Kanetkar, S.B. Ogale, V.G. Bhide, Phys. Rev. Lett. **58**, 238 (1987)
2. B.G. Ershov, A. Henglein, J. Phys. Chem. **97**, 3434 (1993)
3. J. Neddersen, G. Chumanov, T.M. Cotton, Appl. Spectrosc. **47**, 1959 (1993)

4. F. Mafuné, J. Kohno, Y. Takeda, T. Kondow, H. Sawabe, J. Phys. Chem. B **104**, 8333 (2000)
5. C.H. Liang, Y. Shimizu, T. Sasaki, N. Koshizaki, J. Phys. Chem. B **107**, 9220 (2003)
6. C.H. Liang, Y. Shimizu, T. Sasaki, N. Koshizaki, J. Mater. Res. **19**, 1551 (2004)
7. C.H. Liang, Y. Shimizu, M. Masuda, T. Sasaki, N. Koshizaki, Chem. Mater. **16**, 963 (2004)
8. S.I. Dolgaev, A.V. Simakin, V.V. Voronov, G.A. Shafeev, F. Bozon-Verduraz, Appl. Surf. Sci. **186**, 546 (2002)
9. L. Yang, P.W. May, L. Yin, J.A. Smith, K.N. Rosser, J. Nanopart. Res. **9**, 1181 (2007)
10. N. Takada, T. Sasaki, K. Sasaki, Appl. Phys. A **93**, 833 (2008)
11. Y. Ishikawa, Y. Shimizu, T. Sasaki, N. Koshizaki, Appl. Phys. Lett. **91**, 161110 (2007)
12. F. Mafuné, J.Y. Kohno, Y. Takeda, T. Kondow, J. Phys. Chem. B **106**, 8555 (2002)
13. H. Usui, T. Sasaki, N. Koshizaki, J. Phys. Chem. B **110**, 12890 (2006)
14. K. Saitow, T. Yamamura, T. Minami, J. Phys. Chem. C **112**, 18340 (2008)
15. M.W. Mortensen, P.G. Sorensen, O. Bjorkdahl, M.R. Jensen, H.J.G. Gundersen, T. Bjornholm, Appl. Radiat. Isot. **64**, 315 (2006)
16. A. Sinha, T. Mahata, B.P. Sharma, J. Nucl. Mater. **301**, 165 (2002)
17. K.E. Lee, C.O. Kim, M.J. Park, J.H. Kim, Phys. Status Solidi B **241**, 1637 (2004)
18. A.O. Sezer, J.I. Brand, Mater. Sci. Eng. B **79**, 191 (2001)
19. T. Ohyanagi, A. Miyashita, K. Murakami, O. Yoda, Jpn. J. Appl. Phys. Part 1 **33**, 2586 (1994)
20. F. Mafuné, J. Kohno, Y. Takeda, T. Kondow, J. Phys. Chem. B **107**, 12589 (2003)
21. V. Amendola, M. Meneghetti, Phys. Chem. Chem. Phys. **11**, 3805 (2009)
22. R.D. Lide, *Handbook of Chemistry and Physics*, 81st edn. (CRC, Boca Raton, 2000)
23. E.J.W. Verwey, J.T.G. Overbeek, *Theory of the Stability of Lyophobic Colloids* (Elsevier, Amsterdam, 1948)
24. K. Kimura, J. Colloid Interface Sci. **183**, 607 (1996)
25. T. Tsuji, T. Hamagami, T. Kawamura, J. Yamaki, M. Tsuji, Appl. Surf. Sci. **243**, 214 (2005)
26. V. Amendola, M. Meneghetti, J. Mater. Chem. **17**, 4705 (2007)